Experimental study of local scour around T-shaped spur dike in a meandering channel

Ravi Prakash Tripathi and K. K. Pandey

ABSTRACT

A spur dike is mainly constructed as a river-training structure and is primarily used to prevent bank erosion. The restriction to flow caused by the construction of a spur dike promotes local scour around the structure. In the case of a dike placed in a channel bend, the scour becomes more aggressive. The literature review found that the research work related to local scour around a spur dike located in a meandering channel is very limited or minimal. Therefore, an experimental investigation was conducted to study the local scour process around a T-shaped spur dike placed at different locations along the outer bank (or concave) of a reverse-meandering channel. Non-dimensionalized empirical equations for temporal and maximum local scour depth were developed as the function of the Froude number of approach flow and spur dike location. It is observed that local scour around the dike increases with the increase in Froude number and location in the meander (measured from the entry to meander). The formulation for the maximum scour depth was further evaluated with the experimental data related to the 180° bend, from literature, and it was found that the proposed equation's application is very much limited.

Key words | bank erosion, bend, local scour, meander, river training structure, spur dike

Ravi Prakash Tripathi
K. K. Pandey (corresponding author)
Department of Civil Engineering,
Indian Institute of Technology (BHU),
Varanasi 221005,
India
E-mail: *kkp.civ@iitbhu.ac.in*

HIGHLIGHTS

- Scour process is studied around T-shaped spur dike located in reverse meandering channel.
- Various factors affecting scour such as Froude number of approach flow, time of scouring, and spur dike have been evaluated and studied in detail.
- Empirical relations have been developed to estimate temporal and maximum scour depth.
- Some experimental observations regarding flow pattern and bed topography has been discussed.

NOTATION

V	approach flow velocity
W	channel width
L	length of spur dike
R_c	central radius of the bend
S_0	bed slope
d_s, d_{sm}	temporal and maximum scour depth respectively
d_{50}	median grain size
g	acceleration due to gravity
l	wing length of spur dike
t, t_e	time of scouring and time taken to reach maximum scour depth respectively
y	approach flow depth
α	angle of spur dike with bank

doi: 10.2166/ws.2020.331

μ dynamic viscosity of the fluid
ρ_s density of sediment
$\varnothing$ friction angle of sediment
θ location of spur dike in the bend

INTRODUCTION

A spur dike is a hydraulic structure protruding outward from the bank into the channel, and is primarily used as a river-training structure. It deviates the current or flow stream from the bank and hence safeguards the bank from erosion. The restriction to flow caused by the spur dike increases the depth of the main channel (upstream). It enables easy navigation, ensures adequate water supply and uniform flow discharge, and promotes aquatic ecosystems. In the case of a spur dike constructed in a channel bend, it prevents the lateral migration of the outer bank.

In general, the spur dike restricts the flow in the channel, and hence distorts the flow field around itself. This distortion in the flow field (or current field) creates high turbulence in the region around the structure. The presence of boundary layers, along with adverse pressure, complicates the flow characteristics around the spur dike. It results in significant scouring around the structure. Hence, it becomes essential to evaluate the local scour (or maximum scour) around the spur dike or other hydraulic structures (Pandey *et al.* 2018b, 2018c, 2019a, 2019b; Singh *et al.* 2019; Pu *et al.* 2020). Significant researches like Chabert & Engeldinger (1956), Gill (1972), Chiew (1984), Kothyari & Ranga Raju (2001), Melville (1992), Kwan & Melville (1994), Pandey *et al.* (2016), Pu & Lim (2014), Pu *et al.* (2018), Pandey *et al.* (2020a, 2020b), Choufu *et al.* (2019); Pourshahbaz *et al.* (2020), Singh *et al.* (2020) and so on, had been done in the past, related to the local scour around the hydraulic structures such as bridge piers, abutments, and so on, located in the straight channel. The various factors or parameters that influence the local scour around the structure have been studied in the past. These parameters include the geometry of channel and spur dike, approach flow condition, fluid characteristics, properties of bed sediments, and so on. A detailed discussion on the influencing factors or parameters can be collectively found in Zhang & Nakagawa (2008), and Pandey *et al.* (2018a).

In case of the spur dike located in a channel bend, the complexity of flow patterns around the structure increases manifold and hence the scour around it. The complexity arises due to spiral flow, transverse rotational flow, and secondary flow caused by the centrifugal force (Pandey *et al.* 2018a). In general, the outer bank is subjected to scour while the inner bank is subjected to sediment deposition, which gradually transports downstream to form small ridges (Fazli *et al.* 2008; Ghodsian & Vaghefi 2009; Vaghefi *et al.* 2009). It has been observed by many researchers like Fazli *et al.* (2008), Ghodsian & Vaghefi 2009, and so on that the scour hole extends to the inner bank when the length of the spur dike reaches 20% of the channel width. Fazli *et al.* (2008) conducted an experimental study on the scour and flow field around a straight spur dike placed in a 90° flume bend and reported that the maximum scour depth increases as the location of structure shifts towards the exit of the bend (from the entry to the bend). Fazli *et al.* (2008) further concluded that the maximum scour depth increases with the increase in the Froude number of the approach flow and spur dike location. Similar results were also reported by Masjedi *et al.* (2010a, 2010c, 2011), and Rashedipoor *et al.* (2012) for a spur dike located in a 180° channel bend. Vaghefi *et al.* (2012) conducted an experimental investigation to study the scour around a T-shaped spur dike placed in a 90° bend and observed two main scour holes; one forms upstream, near the nose of the wing of the spur dike, and the other forms downstream at a distance from the structure. The amount of scour upstream of the T-shaped spur dike is much higher than that at its downstream (Vaghefi *et al.* 2009). For a constant width of channel, Vaghefi *et al.* (2012) reported that the maximum scour depth increases with a decrease in l/L and R_c/W, where W and R_c are the channel width and central radius of the bend respectively; L, and l are the length and the wing length of the spur dike respectively. For the spur dike located in a 180° bend, similar conclusions were made by researchers such as Masjedi *et al.* (2010a, 2010b, 2010c, 2011) and Rashedipoor *et al.* (2012). For a T-shaped spur dike placed in a 90° channel bend, Vaghefi *et al.* (2012) established an empirical equation for maximum scour dimensions, as a function of l/L, R_c/W, V/V_c, and the spur dike location. Here, V is the approach flow velocity and V_c is the critical flow velocity. Similarly, Masjedi *et al.* (2010a, 2010b, 2010c,

2011) proposed empirical equations for several types of spur dikes located in a 180° channel bend. Daneshfaraz *et al.* (2019) conducted an experimental study of the screen as an energy dissipator under movable bed condition and reported a significant reduction in bed scour in the case of a screen with 50% porosity.

The numerical modeling in the field of Computational Fluid Dynamics (CFD) has significantly improved over the past decade. Chen & Li (1989), Tingsanchali & Maheswaran (1990), Molls *et al.* (1995), Mayerle *et al.* (1995), Peng (2004), Tang *et al.* (2006), Yazdi *et al.* (2010), and so on, extensively used various numerical models such as turbulence model, Large Eddy Simulation (LES), and so on to study the flow characteristics in the channel. Oslen (2018) and his associates developed the SSIIM model (Sediment Simulation in Intakes with a Multiblock option) to model the sediment transport in the numerical model. The model solves the Navier-Stoke equation with *k*-e epsilon model. By default, the model uses a semi-implicit method for pressure-linked equations to compute the pressure term in the equation (Oslen 1999, 2000, 2001). Vaghefi and his associates (Vaghefi *et al.* 2015, 2016, 2017a, 2017b) extensively used the SSIIM model to study the flow characteristics and scour process around a T-shaped spur dike placed in a 90° channel bend. For further detail, the readers are recommended to refer to these references. Daneshfaraz *et al.* (2015) implemented a three-phase simulation (air, water, sediment) based on the VOF model to study the flow field and scour around a T-shaped spur dike located in a 90° arc. It was reported that the scour at the outer arc or bank increases with an increase in discharge or volume rate.

The literature survey indicates that the majority of previous works (or studies) on the scour around the spur dike were performed either in the straight reach of the channel or a regular channel bend; that is, 90° and 180° bends. Minimal focus is given to other channel types such as sinusoidal channels, meandering channels, and so on. In this paper, work is extended to examine the flow field, and the local scour around the T-shaped spur dike placed in a reverse meandering channel under subcritical flow conditions. The influence of parameters on local scour such as the Froude number of approach flow, location of the structure in the meander, and time duration are studied. Further, experimental data are used to formulate non-dimensional empirical equations for temporal and maximum local scour depth. The formulation for maximum scour depth is further tested with the experimental data from other researches (related to 180° channel bends) to check the extension of its application.

EXPERIMENTAL SETUP

The experiment was conducted in a meandering channel with a rectangular cross-section and two consecutive bends of reverse order, as shown in Figure 1. These consecutive bends were connected with the straight inlet and outlet channels, each of 6.0 m length. The width of channel cross-section was kept uniform, equal to 1.0 m. The central radius of both bends was designed as 1.0 m. The bend is categorized as a sharp bend because of the value, R_c/W; that is, the relative curvature was 1.0. The central angle of the bend was kept at 180° for the maximum deflection of flow and hence to generate maximum development of secondary circulation. The floor and the wall of the rectangular

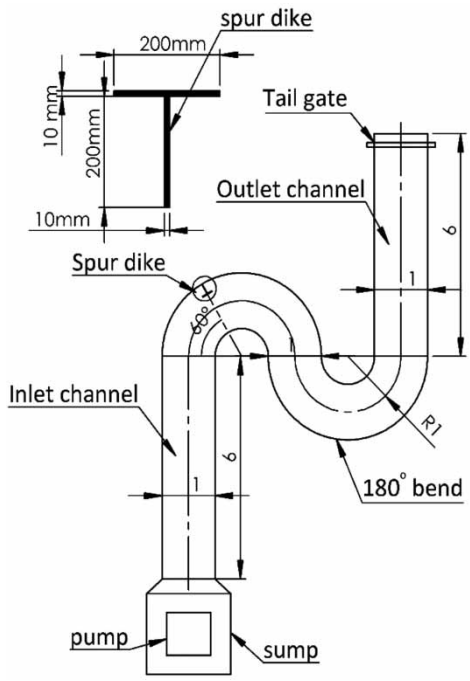

Figure 1 | A schematic diagram of the experimental setup.

channel were made impermeable by plastering with cement mortar. A 0.25 m thick layer of bed sediment, having median diameter, $d_{50} = 2$ mm and standard deviation, $\sigma_g = 1.8$ was uniformly distributed throughout the channel. The spur dike, having a thickness of 10 mm and height of 200 mm, was made of perspex sheet and was placed perpendicular to the curvature of the flume bend. The length and the wing length of the spur dike were taken as 20% (200 mm) of the width of the channel.

A tailgate was installed at the end of the outlet channel to regulate the flow depth in the channel. The water coming out from the exit of the main channel was carried by a side-channel, which was equipped with a sharp-crested rectangular weir to measure the discharge. A centrifugal pump was connected to the setup that carried water back to the sump well. At the beginning of each experimental run, the channel bed was leveled using a scrapper, and the flume was filled with water up to the required depth. Before the pump was started, an initial set of channel bed elevation values in the region where scour was expected to occur was collected. After the experiment was completed, water in the flume was drained out slowly, causing very minimal disturbance to the channel bed topography, and the flume was then left to dry.

Pictures of the scour (or bed) topography in the region near the spur dike were taken. A point gauge, having an accuracy of ± 0.01 mm, was used to measure the bed elevation and the scour depth. The experiment was conducted for the spur dike located in the first bend at the angles of 30°, 60°, 120°, and 150° (measured from the entry to the bend). A schematic diagram for the spur dike placed at 60° is shown in Figure 1. For each location, the experiment runs for four different discharge values (or Froude number). It should be noted that the experiment was conducted under clear-water condition and sub-critical approach flow condition. A preliminary experimental run was conducted for five hours, and it was found that the change in bed elevation at the location of maximum scour becomes negligible. A similar observation is made by Masjedi *et al.* (2010a, 2010b, 2010c, 2011). Therefore, the observation duration of each experimental run was kept at 3 hours (or 180 minutes). The experimental setup for the spur dike located at 60° (measured from the entry of the channel) in the bend is shown in Figure 2.

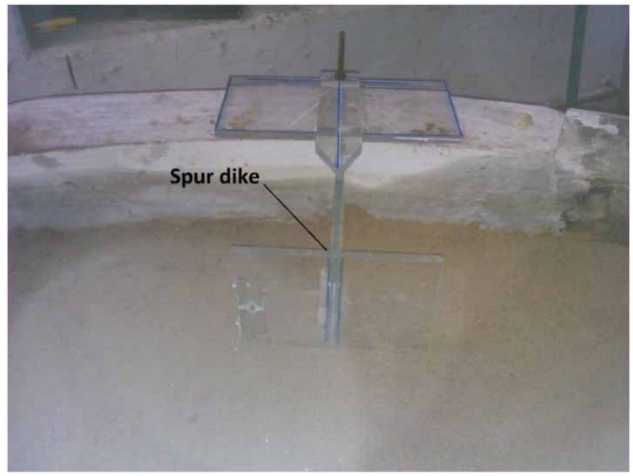

Figure 2 | An experimental setup for the spur dike located at 60°.

GENERAL EQUATION

The local scour around the T-shaped spur dike placed in a channel bend depends on: (1) geometry of the channel (width, radius, and bed-slope); (2) spur dike characteristics (its length and wing length, inclination with the bank, and location in the channel); (3) approach flow conditions (depth, discharge rate and velocity of flow); (4) properties of the bed sediment (specific gravity, grain size, friction angle); (5) properties of the flowing fluid (its density and viscosity); and (6) time duration. Hence, the scour depth can be expressed as

$$d_s = f(L, l, \alpha, \theta, y, W, S_0, V, g, d_{50}, R_c, \rho_s, \varnothing, \rho, \mu, t, t_e) \quad (1)$$

where d_s is temporal (time-varying) scour depth; L, l are the length and the wing length of the spur dike respectively; α is the angle of the spur dike with the bank; θ is the location of the spur dike in the bend measured from the entry to the bend; y and V are the depth and velocity of the approach flow; W is the channel width; S_0 is the bed slope; g is gravitational acceleration; d_{50} is median grain size; R_c is the central radius of the bend; ρ_s is the density of sediment; μ is the dynamic viscosity of the flowing fluid; $\varnothing$ is the frictional angle of sediment; t is the time of scouring; and t_e is the time taken to reach maximum (or equilibrium) scour depth.

Using dimensional analysis, Equation (1) can be written in a non-dimensional form as

$$\frac{d_s}{y} = f\left(\mathrm{Re}, \mathrm{Fr}, \frac{\theta}{180}, \alpha, S_0, \varnothing, \frac{L}{R_c}, \frac{d_{50}}{y}, \frac{L}{W}, \frac{l}{L}, \frac{L}{d_{50}}, \frac{\rho_s}{\rho}, \frac{R_c}{W}, \frac{t}{t_e}\right) \quad (2)$$

Here, Fr, and Re are the Froude number and the Reynold's number related to approach flow respectively. In this study, it is assumed that Fr, θ (in degrees) and t/t_e are the only influencing parameters as these are the only parameters that change during the experimental run (discussed in the previous section); all other parameters are either constants or assumed to have a negligible effect on scouring phenomenon. Therefore, Equation (2) can be simplified as:

$$\frac{d_s}{y} = f\left(Fr, \frac{\theta}{180}, \frac{t}{t_e}\right) \quad (3)$$

RESULTS AND DISCUSSION

Flow characteristics in general

To visualize the surface flow structure around the spur dike at equilibrium scour condition, tracers were used. As expected, the restriction to flow caused by the spur dike results in the formation of three different zones in the region surrounding the spur dike. These three zones are termed as the main channel zone, an embayment zone, and a mixing zone (Zhang & Nakagawa 2008; Pandey *et al.* 2018a). The main channel zone spans from the wing of the spur dike to the opposite inner bank of the channel, the embayment zone located between the wing of the spur dike and the outer bank from where the structure protruded, and the mixing zone between the two. It was observed that when the flow approaches the spur dike, a strong inward circulation is generated. With the increase in the spur dike's location from the entry of bend, the length of flow separation and, hence, the embayment zone increases. It occurs due to the diversion of streamline flow caused by the curvature of the bend. The flow velocity was found to be decreasing in the embayment zone. Here, the tracers representing the central area of the embayment were observed to be diverted in three directions; downstream, upstream, and towards the main channel. Hence, it can be concluded that the flow pattern around the spur dike is very complicated and strongly three-dimensional. It may occur due to the formation of the degraded bed surface.

Bed topography

The artificial narrowing created in the main channel caused by the spur dike results in flow disturbances around the structure. It was observed that two main scour holes form; one upstream forms near the nose (or wing of the spur dike); and the other downstream forms in the embayment area at a distance from the spur dike, as can be seen in Figure 3. As the location of the spur dike shifts to the end of the first bend, the scour area upstream stretches along the wing of the spur dike and merges with the scour area downstream. The sediment erosion in the embayment area suggests that there are strong return currents generated in the area. Because of the diverted flow generating at the head of the spur dike, various local scours form in front of the structure. These scour holes started forming as soon as the pump was started. In general, it was observed that the sediment erosion takes place at the outer bank while deposition occurs at the inner bank. In the case of a spur dike placed at $\theta = 30^\circ$, the deposition occurs nearly throughout the length of the inner bank (of the first bend), as shown in Figure 3(a). A similar observation was also reported by Fazli *et al.* (2008) and Vaghefi *et al.* (2009). For $\theta = 120^\circ$ and 150°, the scour area extends to the main channel (closer to the inner bank) as well, shown in Figure 3(b). In case of $\theta = 120^\circ$ and 150°, the increase in turbulent and secondary flow caused due to change in the curvature of the bend results in severe scour in the main channel, both upstream and downstream, resulting in extensive bed degradation, as shown in Figure 3(b). It is interesting to note that the scour area formed upstream is bounded and located far from the structure. It might occur due to the sharp change in the channel's curvature, creating a high secondary and spiral flow, followed by backwater formation caused by the spur dike resulting in the generation of a high turbulence region at the upstream side. The increased velocity of

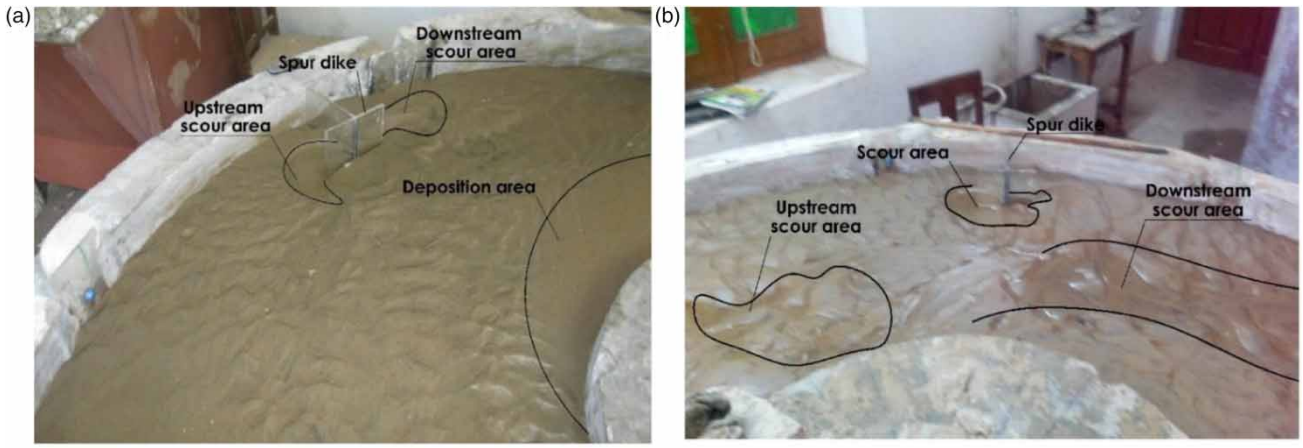

Figure 3 | Bed topography for spur located at (a) $\theta = 30^{\circ}$ and (b) $\theta = 120^{\circ}$.

diverted flow associated with high turbulence downstream results in scouring near the tip of the spur dike's wing, which extends in an elongated fashion or pattern. Since only tracer has been used to study the surface flow characteristics, the exact reason behind such scours is not identified and, hence, can be treated as an experimental limitation. A highly advanced setup to observe the flow field is required.

It was seen that with increasing discharge (or Froude number), flow is attracted towards the spur dike, which causes scour near the nose of the wing (upstream). With the increase in Froude number, general scour in the channel reduces and shifts towards the spur dike, while the main scour hole depth increases. A general scour contour for $Fr = 0.35$ and $Fr = 0.50$ is shown in Figure 4 for a spur dike placed at $\theta = 30^{\circ}$. From Figure 4, it can be seen that the overall bed elevation in the main channel zone decreases with the increase in the Froude number (from 0.35 to 0.50). From Figure 4(b) it can be seen that at a higher Froude number, the local scour hole upstream of the spur dike extends to merge with the scour hole downstream. This phenomenon might be the consequence of the formation of large vortices around the wing of the spur dike.

Temporal and maximum scour depth

In general, scour increases rapidly in the earlier stage of its development and then gradually grows at a decreased rate, reaching its maximum value after some time. The time-varying scour depth for each location of spur dike in the channel is shown in Figure 5. The figure shows that the considerable amount of scour depth (nearly 90% of maximum scour

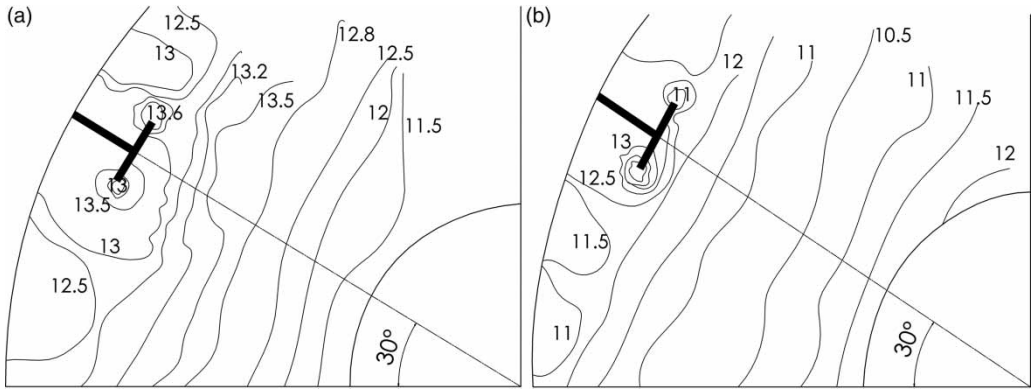

Figure 4 | Scour contour around spur dike located at $\theta = 30^{\circ}$ for (a) $Fr = 0.35$ and (b) $Fr = 0.50$.

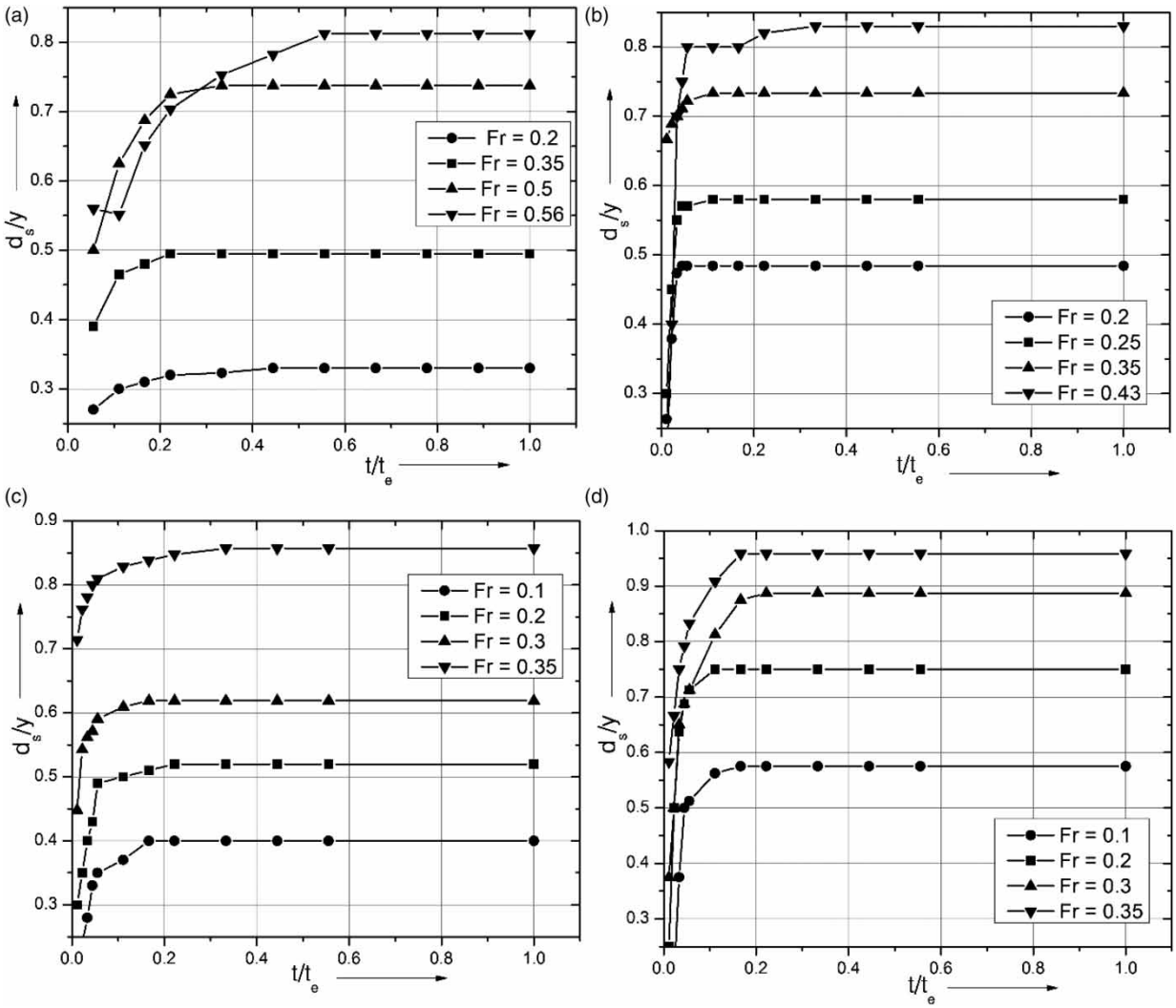

Figure 5 | Temporal scour depth variation for spur dike located at $\theta = 30°$, 60°, 120°, and 150° respectively.

depth) is reached within 20% of experimental duration except in few cases. A similar finding was made by several other researchers, such as Pu & Lim (2014). The temporal scour depth variation shows logarithmic incremental behavior (Coleman *et al.* 2003; Kothyari *et al.* 2007). From Figure 5(a), it is interesting to note that the transition stage (curvy region) of scour development is well defined and steady (or smooth) for a spur dike located at $\theta = 30°$. The transition stage becomes sharp (or unsteady) as the location of the spur dike shifts towards the end of the first bend. It can be concluded from the graph that for each location of the spur dike, the temporal scour depth increases with an increase in Froude number.

For a spur dike located at $\theta = 120°$ and 150°, local scour was observed to be very high even for approach flow with a low Froude number. It was found that for $\theta = 150°$ and $Fr = 0.10$, the maximum non-dimensionalized scour-depth value is 0.58, which is close to the value for $\theta = 60°$ and $Fr = 0.25$. In this case, the region around the bend is most affected by scouring, as shown in Figure 3(b). This may occur due to change in the curvature of the meandering channel (or inflection point) downstream. From Figure 5, it can be concluded that for a constant value of Froude number (i.e., $Fr = 0.20$ and 0.35), the initial growth rate of scour depth increases as the spur dike shifts towards the end of the first bend. In addition, the maximum scour depth also increases

with an increase in the Froude number and location of the spur dike (see Figure 6 and Figure 7, respectively).

Mathematical formulation for temporal and maximum scour depth

Since the scour depth shows logarithmic incremental variation, Equation (3) in non-dimensional form can be written in the following empirical form as

$$\frac{d_s}{y} = a \cdot Fr^b \left[\frac{\theta}{180}\right]^c ln\left[\frac{t+t_e}{t_e}\right] \quad (4)$$

The constants a, b, c are determined by the method of best-fit using the experimental data. The resulting equation comes out as

$$\frac{d_s}{y} = 2.747 \cdot Fr^{0.574} \left[\frac{\theta}{180}\right]^{0.381} ln\left[\frac{t+t_e}{t_e}\right] \quad (5)$$

The maximum scour depth, d_{sm} is reached at $t = t_e$. And hence, Equation (5) is reduced to

$$\frac{d_{sm}}{y} = 1.904 \cdot Fr^{0.574} \left[\frac{\theta}{180}\right]^{0.381} \quad (6)$$

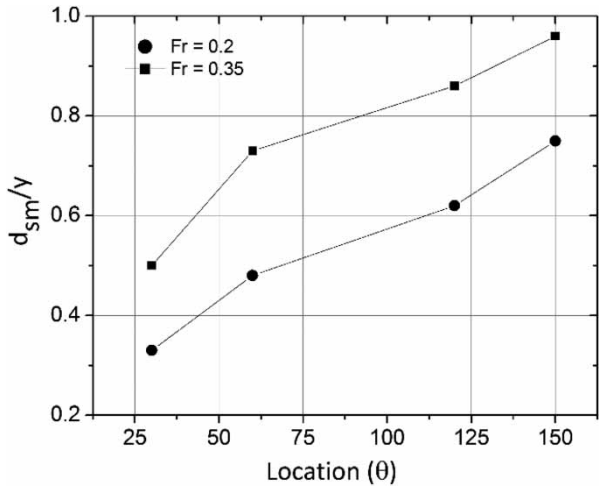

Figure 7 | Variation of d_{sm}/y vs. θ.

Equations (5) and (6) show self-similarity. Equation (6) is used to estimate the maximum scour depth and then compared with the measured data. The developed equation for scouring shows good accuracy when compared with experimental data, having $R^2 = 0.895$ and percentage error ranging between 1.28% and 18.33%, as can be seen from Figure 8. Therefore, it can be expected that the relationship derived is good for the given range of Froude numbers.

To check the applicability of the proposed equation to other conditions, experimental data from Masjedi *et al.* (2010b, 2010c, 2011) were used. Masjedi *et al.* (2010b, 2010c) conducted an experimental investigation on scour around

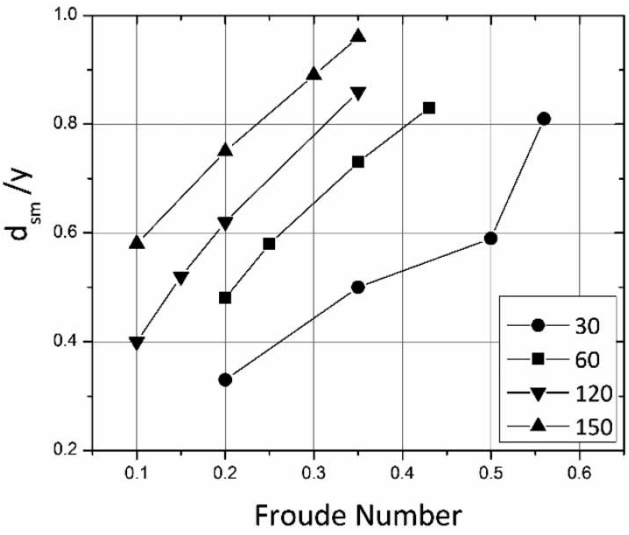

Figure 6 | Variation of d_{sm}/y with Froude number for different locations of spur dike.

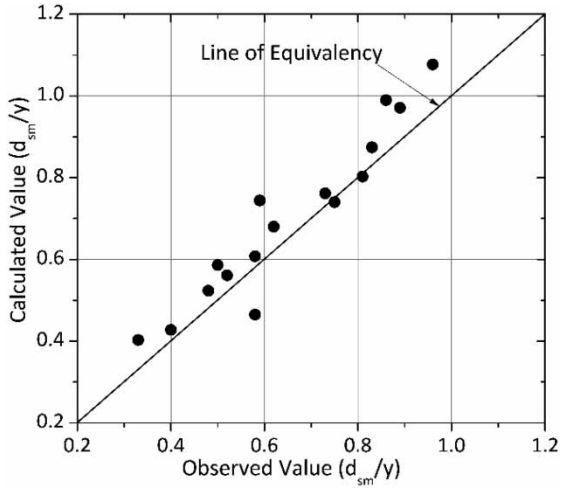

Figure 8 | Comparison of calculated and observed value of maximum scour depth.

a T-shaped spur dike placed in a 180° bend. Similarly, Masjedi *et al.* (2011) experimented in a 180° channel bend to study the scour process around an L-shaped spur dike. This attempt was made by assuming that the downstream flow characteristics have a negligible effect on maximum scour depth. Since the bend angle in all the three cases is 180°, it is presumed that the proposed equation could give reasonable results. It was found that the proposed equation overestimated the maximum scour depth, nearly by an average factor of 1.19, 1.41, and 2.2 for Masjedi *et al.* (2010b, 2010c, 2011) respectively (see Figure 9). This may occur due to various other influencing parameters that are assumed to be constant or have a negligible effect. Therefore, it is recommended that various other parameters are encompassed in developing such empirical equation.

CONCLUSION

The experiment was set up to investigate the flow field and scour depth in the area surrounding a spur dike placed at various locations in a reverse meandering channel. The reverse meandering channel enables maximum deflection of the flow field, and hence generates high turbulence and secondary flow condition to simulate the maximum amount of scour around a spur dike. This study would be helpful as an engineering application in a river channel where the last stage of meandering is almost reached (i.e. before the formation of an ox-bow lake). Vortex flow was observed at the beginning of each experimental run, due to which a secondary current was created. The secondary flow transports the sediments towards the convex side (inner bank), creating a few dunes near the inner wall. It can be concluded that the local scour holes formed might extend to the river banks in case of a high flow discharge rate (or Froude number). This could be attributed to the existence of return currents towards the river banks generated when the flow is diverted from the heads of the spur dikes. This further resulted in the sound degradation of the main channel near the spur dike. From an engineering perspective, this is a significant drawback. If appropriate countermeasures are not taken, then both the river bank and structure are at risk. It may lead to failure and then collapse of the structure. It was observed that the maximum scour depth increases with an increase in the Froude number and location of the spur dike from the entry of bend. The temporal variation of scour depth with time shows a logarithmic trend. Empirical relations for temporal and maximum scour depth are established as a function of the Froude number, and the position of the structure in the bend. The developed equation shows good accuracy when compared with (own) experimental data. However, it overestimates the maximum scour depth for experimental data (related to 180° channel bend) from literature. This discrepancy could be the result of negligence of several parameters that affect the scour depth. In addition, the range of the Froude number of the approach flow is kept narrow due to experimental setup constraints. In the future scope of studies, it is advised to incorporate various parameters that influence the scour, such as the dimensions of the spur dike, channel parameters, and so on, and to run experiments for a wide range of Froude number. In this study, only tracers were used to carry out a qualitative assessment of the surface flow field, which is very limited to a greater extent. In future studies, it is recommended to include a quantitative assessment of the flow field around the structure. The study can be further carried out for simultaneous positioning of a spur dike at different locations on the concave side of the meandering channel. At a later stage, the study can also be incorporated with numerical investigation or modeling.

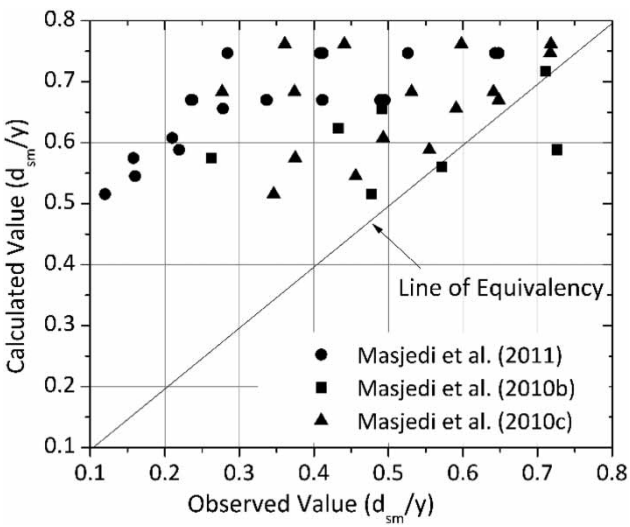

Figure 9 | Comparison of calculated and observed value of maximum scour depth (from other researches).

ACKNOWLEDGEMENTS

Thanks to IIT(BHU) for providing me the opportunity to perform the experiment.

DATA AVAILABILITY STATEMENT

All relevant data are included in the paper or its Supplementary Information.

REFERENCES

Chabert, J. & Engeldinger, P. 1956 Study of scour around bridge piers. *Rep. Prepared for the Laboratoire National D'Hydraulique*, Paris, France.

Chen, N. S. & Li, C. H. 1989 Numerical solution of the flow around a spur dike with turbulent model. *Journal of Nanjing Hydraulic Research Institute* **3**, 11–23.

Chiew, Y. M. 1984 *Local Scour at Bridge Piers*. *Doctoral Dissertation*. ResearchSpace@ Auckland.

Choufu, L., Abbasi, S., Pourshahbaz, H., Taghvaei, P. & Tfwala, S. 2019 Investigation of flow, erosion, and sedimentation pattern around varied groynes under different hydraulic and geometric conditions: a numerical study. *Water* **11** (2), 235.

Coleman, S. E., Lauchlan, C. S. & Melville, B. W. 2003 Clear-water scour development at bridge abutments. *Journal of Hydraulic Research* **41** (5), 521–531.

Daneshfaraz, R., Ghaderi, A. & Ghahremanzadeh, A. 2015 An analysis of flowing pattern around T-shaped spur dike at 90 arc, based on Fluent and Flow-3D models. *International Bulletin of Water Resources and Development* **3** (3), 1–9.

Daneshfaraz, R., Sadeghfam, S. & Tahni, A. 2019 Experimental investigation of screen as energy dissipators in the movable-bed channel. *Iranian Journal of Science and Technology, Transactions of Civil Engineering* **44**, 1237–1246.

Fazli, M., Ghodsian, M. & Neyshabouri, S. A. A. S. 2008 Scour and flow field around a spur dike in a 90° bend. *International Journal of Sediment Research* **23** (1), 56–68.

Ghodsian, M. & Vaghefi, M. 2009 Experimental study on scour and flow field in a scour hole around a T-shape spur dike in a 90° bend. *International Journal of Sediment Research* **24** (2), 145–158.

Gill, M. A. 1972 Erosion of sand beds around spur dikes. *Journal of the Hydraulics Division* **98** (hy9).

Kothyari, U. C. & Ranga Raju, K. G. 2001 Scour around spur dikes and bridge abutments. *Journal of Hydraulic Research* **39** (4), 367–374.

Kothyari, U. C., Hager, W. H. & Oliveto, G. 2007 Generalized approach for clear-water scour at bridge foundation elements. *Journal of Hydraulic Engineering* **133** (11), 1229–1240.

Kwan, R. T. & Melville, B. W. 1994 Local scour and flow measurements at bridge abutments. *Journal of Hydraulic Research* **32** (5), 661–673.

Masjedi, A., Bejestan, M. S. & Moradi, A. 2010a Experimental study on the time development of local scour at a spur dike in a 180°-flume bend. *Journal of Food, Agriculture & Environment* **8** (2), 904–907.

Masjedi, A., Bejestan, M. S. & Rahnavard, P. 2010b Experimental study on the time development of local scour on around single T-shape spur dike in a 180-degree flume bend. *Research Journal of Environmental Sciences* **4** (6), 530–539.

Masjedi, A., Dehkordi, V., Alinejadi, M. & Taeedi, A. 2010c Experimental study on scour depth in around a t-shape spur dike in a 180-degree bend. *World Applied Sciences Journal* **10** (10), 1146–1152.

Masjedi, A., Akbari, I. & Abyar, H. 2011 Evaluating scour at L-shape spur dike in a 180-degree bend. *World Applied Sciences Journal* **15** (12), 1740–1745.

Mayerle, R., Wang, S. S. Y. & Toro, F. M. 1995 Verification of a three-dimensional numerical model simulation of the flow in the vicinity of spur dikes. *Journal of Hydraulic Research* **33** (2), 243–256.

Melville, B. W. 1992 Local scour at bridge abutments. *Journal of Hydraulic Engineering* **118** (4), 615–631.

Molls, T., Chaudhry, M. H. & Khan, K. W. 1995 Numerical simulation of two-dimensional flow near a spur-dike. *Advances in Water Resources* **18** (4), 227–236.

Oslen, N. R. B. 1999, 2000, 2001 *Computational Fluid Dynamics in Hydraulic and Sedimentation Engineering*. Class Notes. Department of Hydraulic and Environmental Engineering, Norwegian University of Science and Technology, Norway

Oslen, N. R. B. 2018 *A Three-Dimensional Numerical Model for Simulation of Sediment Movement in Water Intakes with Multi-Block Option*. User's Manual. Department of Hydraulic and Environmental Engineering, Norwegian University of Science and Technology, Norway.

Pandey, M., Ahmad, Z. & Sharma, P. K. 2016 Estimation of maximum scour depth near a spur dike. *Canadian Journal of Civil Engineering* **43** (3), 270–278.

Pandey, M., Ahmad, Z. & Sharma, P. K. 2018a Scour around impermeable spur dikes: a review. *ISH Journal of Hydraulic Engineering* **24** (1), 25–44.

Pandey, M., Sharma, P. K., Ahmad, Z., Singh, U. K. & Karna, N. 2018b Three-dimensional velocity measurements around bridge piers in gravel bed. *Marine Georesources & Geotechnology* **36** (6), 663–676.

Pandey, M., Sharma, P. K., Ahmad, Z. & Singh, U. K. 2018c Experimental investigation of clear-water temporal scour variation around bridge pier in gravel. *Environmental Fluid Mechanics* **18** (4), 871–890.

Pandey, M., Lam, W. H., Cui, Y., Khan, M. A., Singh, U. K. & Ahmad, Z. 2019a Scour around spur dike in sand–gravel mixture bed. *Water* **11** (7), 1417.

Pandey, M., Chen, S. C., Sharma, P. K., Ojha, C. S. P. & Kumar, V. 2019b Local scour of armor layer processes around the circular pier in non-uniform gravel bed. *Water* **11** (7), 1421.

Pandey, M., Azamathulla, H. M., Chaudhuri, S., Pu, J. H. & Pourshahbaz, H. 2020a Reduction of time-dependent scour around piers using collars. *Ocean Engineering* **213**, 107692.

Pandey, M., Valyrakis, M., Qi, M., Sharma, A. & Lodhi, A. S. 2020b Experimental assessment and prediction of temporal scour depth around a spur dike. *International Journal of Sediment Research* **36** (1), 17–28.

Peng, J. 2004 *Flow and Local Scour Around Spur-Dike*. The Yellow River Press Publications, Zheng Zhou, China.

Pourshahbaz, H., Abbasi, S., Pandey, M., Pu, J. H., Taghvaei, P. & Tofangdar, N. 2020 Morphology and hydrodynamics numerical simulation around groynes. *ISH Journal of Hydraulic Engineering* 1–9.

Pu, J. H. & Lim, S. Y. 2014 Efficient numerical computation and experimental study of temporally long equilibrium scour development around abutment. *Environmental Fluid Mechanics* **14** (1), 69–86.

Pu, J. H., Tait, S., Guo, Y., Huang, Y. & Hanmaiahgari, P. R. 2018 Dominant features in three-dimensional turbulence structure: comparison of non-uniform accelerating and decelerating flows. *Environmental Fluid Mechanics* **18** (2), 395–416.

Pu, J. H., Pandey, M. & Hanmaiahgari, P. R. 2020 Analytical modelling of sidewall turbulence effect on streamwise velocity profile using 2D approach: a comparison of rectangular and trapezoidal open channel flows. *Journal of Hydro-Environment Research* **32**, 17–25.

Rashedipoor, A., Masjedi, A. & Shojaenjad, R. 2012 Investigation on scour hole around spur dike in a 180 degree flume bend. *World Applied Sciences Journal* **19** (7), 924–928.

Singh, U. K., Ahmad, Z., Kumar, A. & Pandey, M. 2019 Incipient motion for gravel particles in cohesionless sediment mixtures. *Iranian Journal of Science and Technology, Transactions of Civil Engineering* **43** (2), 253–262.

Singh, R. K., Pandey, M., Pu, J. H., Pasupuleti, S. & Villuri, V. G. K. 2020 Experimental study of clear-water contraction scour. *Water Supply* **20** (3), 943–952.

Tang, X., Ding, X. & Chen, Z. 2006 Large eddy simulations of three-dimensional flows around a spur dike. *Tsinghua Science and Technology* **11** (1), 117–123.

Tingsanchali, T. & Maheswaran, S. 1990 2-D depth-averaged flow computation near groyne. *Journal of Hydraulic Engineering* **116** (1), 71–86.

Vaghefi, M., Ghodsian, M. & Salehi Neyshaboori, S. A. A. 2009 Experimental study on the effect of a T-shaped spur dike length on scour in a 90° -channel bend. *Arabian Journal for Science and Engineering* **34** (2), 337.

Vaghefi, M., Ghodsian, M. & Neyshabouri, S. A. A. S. 2012 Experimental study on scour around a T-shaped spur dike in a channel bend. *Journal of Hydraulic Engineering* **138** (5), 471–474.

Vaghefi, M., Safarpoor, Y. & Hashemi, S. S. 2015 Effects of relative curvature on the scour pattern in a 90° bend with a T-shaped spur dike using a numerical method. *International Journal of River Basin Management* **13** (4), 501–514.

Vaghefi, M., Safarpoor, Y. & Akbari, M. 2016 Numerical investigation of flow pattern and components of three-dimensional velocity around a submerged T-shaped spur dike in a 90° bend. *Journal of Central South University* **23** (11), 2984–2998.

Vaghefi, M., Safarpoor, Y. & Akbari, M. 2017a Numerical comparison of the parameters influencing the turbulent flow using a T-shaped spur dike in a 90° bend. *Journal of Applied Fluid Mechanics* **10** (1), 231–241.

Vaghefi, M., Safarpoor, Y. & Hashemi, S. S. 2017b Effect of T-shaped spur dike on flow separation in a 90° bend using SSIIM model. *Journal of the National Science Foundation of Sri Lanka* **45**, 2.

Yazdi, J., Sarkardeh, H., Azamathulla, H. M. & Ghani, A. A. 2010 3D simulation of flow around a single spur dike with free-surface flow. *International Journal of River Basin Management* **8** (1), 55–62.

Zhang, H. & Nakagawa, H. 2008 *Scour Around Spur Dyke: Recent Advances and Future Researches*. Kyoto University, Kyoto, Japan.

First received 8 August 2020; accepted in revised form 9 November 2020. Available online 19 November 2020